Proc. Natl. Acad. Sci. USA
Vol. 91, pp. 5089–5093, May 1994
Medical Sciences

Mitochondrial creatine kinase: A major constituent of pathological inclusions seen in mitochondrial myopathies

(mitochondrial disorders/encephalomyopathy/"ragged-red" fibers/mitochondrial crystals)

AD M. STADHOUDERS*†, PAUL H. K. JAP*, HANS-PETER WINKLER‡, HANS M. EPPENBERGER§, AND THEO WALLIMANN§

*Department of Cell Biology and Histology, Faculty of Medical Sciences, University of Nijmegen, P.O. Box 9101, 6500 HB Nijmegen, The Netherlands; ‡Department of Cell Biology, Duke University Medical Center, Durham, NC 27710; and §Institute for Cell Biology, Swiss Federal Institute of Technology, Eidgenössische Technische Hochschule-Hönggerberg, CH-8093 Zürich, Switzerland

Communicated by E. R. Weibel, January 13, 1994

ABSTRACT **Overaccumulation of abnormally organized mitochondria in so-called "ragged-red" skeletal muscle fibers is a morphological hallmark of mitochondrial myopathies, in particular of mitochondrial encephalomyopathies. Characteristic for the abnormal mitochondria is the occurrence of highly ordered crystalline inclusions. Immuno-electron microscopy revealed that these inclusions react heavily with specific antibodies against mitochondrial creatine kinase (Mi-CK). Image processing of selected crystalline inclusions, sectioned along the crystallographic *b*, *c* planes, resulted in an averaged picture displaying an arrangement of regular, square-shaped particles with a central cavity. The overall appearance, dimensions, and symmetry of these building blocks are very reminiscent of single isolated Mi-CK octamers. Taking these findings together, it is concluded that Mi-CK octamers indeed represent the major, if not the only, component of these mitochondrial inclusions.**

The mitochondrial myopathies in which a defect in mitochondrial metabolism is thought to be the primary cause of the disease are clinically, biochemically, and genetically a heterogeneous group of disorders (1–3). For example, biochemical analysis reveals that respiratory chain deficiencies can be absent or vary from isolated defects to combined defects of several complexes of the chain (4, 5). To a varying degree, respiratory chain defects have also been reported in the so-called "encephalomyopathies"—i.e., in *c*hronic *p*rogressive *e*xternal *o*phthalmoplegia (CPEO), in Kearns–Sayre syndrome, in MELAS (mitochondrial *m*yopathy, *e*ncephalopathy, *l*actic *a*cidosis, and *s*troke-like episodes), and in MERRF [*m*yoclonus *e*pilepsy with *r*agged-*r*ed *f*ibers (RR fibers)] syndrome. All of these diseases are characterized by the presence of RR fibers in muscle biopsy specimens (1, 2). Characteristic aspects of the pathology in the RR fibers are an accumulation of abnormal and enlarged mitochondria and the occurrence in these mitochondria of highly ordered crystal-like inclusions, often referred to as "railway-track" or "parking lot" inclusions, within their intermembrane spaces (6, 7).

Using optical diffraction techniques on thin muscle biopsy sections, the mitochondrial inclusions were shown to be true crystals (8). Two distinct types of crystals, type I (Fig. 1*A*) and type II (Fig. 1*B*), can be distinguished on the basis of shape, size, pattern, unit cell dimension, specific location of the crystals in the mitochondrial intermembrane space, and occurrence in different muscle fiber types. Understanding the role of the crystals in relation to the patient's pathology, either in terms of causative dysfunction or of mitochondrial response to a disease, requires a detailed knowledge of their chemical composition. Therefore, the biochemical and immunological nature of these inclusions has been studied using proteolytic digestion, enzyme cytochemistry, and immunogold labeling techniques. In addition, image processing of selected areas of these crystalline inclusions was performed to obtain more detailed structural information concerning the unit cell dimensions of the building blocks of the crystals. Part of these results have been reported in abstract form (9, 10).

MATERIALS AND METHODS

Histochemical Procedures. For digestion experiments and immuno-electron microscopy the muscle biopsy specimens were fixed in a 0.1 M phosphate-buffered paraformaldehyde (2%)/glutaraldehyde (0.1%) mixture for ≈2 hr at 0°C. The tissue blocks were then transferred at room temperature through 50% and 70% ethanol and a mixture of 70% ethanol/LR White resin to pure LR White resin as embedding medium. Polymerization occurred at 50°C for 24–48 hr.

For digestion studies LR White sections were incubated with 1 mg and 10 mg of Pronase P per ml (Polysciences, Eppelheim, Germany) in 10 mM Tris/EDTA buffer or with 0.5 mg and 5 mg of RNase per ml (Sigma) in 10 mM Tris/EDTA buffer for 30 min at 37°C. Thereafter, the specimens were rinsed in Tris/EDTA buffer and contrasted with uranyl acetate and lead citrate.

For immuno-electron microscopy, LR White sections were picked up on nickel grids and blocked for 30 min in 1% bovine serum albumin (BSA) in phosphate-buffered saline (PBS: 130 mM NaCl/3 mM KCl/2 mM KH_2PO_4/8 mM $Na_2HPO_4 \cdot 2H_2O$, pH 7.3). The sections were then washed three times in PBS for 10 min and incubated with the primary antiserum for 30 min at room temperature. Subsequently, they were thoroughly rinsed with PBS and then incubated for 30 min with 1% BSA-diluted (1:400) protein A/10-nm gold complex at room temperature. The sections were then rinsed once in PBS and another three times in distilled water, dried, and double-contrasted with uranyl acetate and lead citrate. The polyclonal antibodies used were raised against cytochrome *c* oxidase [COX R 164, rabbit anti-human heart (dilution 1:50)], cytochrome *c* [(rabbit anti-baboon (R 3020-B3) and rabbit anti-chimpanzee (O148-B5) antibody (dilution 1:300)], and specific rabbit anti-chicken mitochondrial creatine kinase (Mi-CK) (dilution 1:200) (11, 12).

The publication costs of this article were defrayed in part by page charge payment. This article must therefore be hereby marked "*advertisement*" in accordance with 18 U.S.C. §1734 solely to indicate this fact.

Abbreviations: RR fibers, ragged-red fibers; CPEO, chronic progressive external ophthalmoplegia; MELAS, mitochondrial myopathy, encephalopathy, lactic acidosis, and stroke-like episodes; MERRF, myoclonus epilepsy with ragged-red fibers; COX, cytochrome oxidase; CK, creatine kinase; Mi-CK, mitochondrial CK; *P*Cr, phosphocreatine; GPA, β-guanidinopropionic acid.

†To whom reprint requests should be addressed.

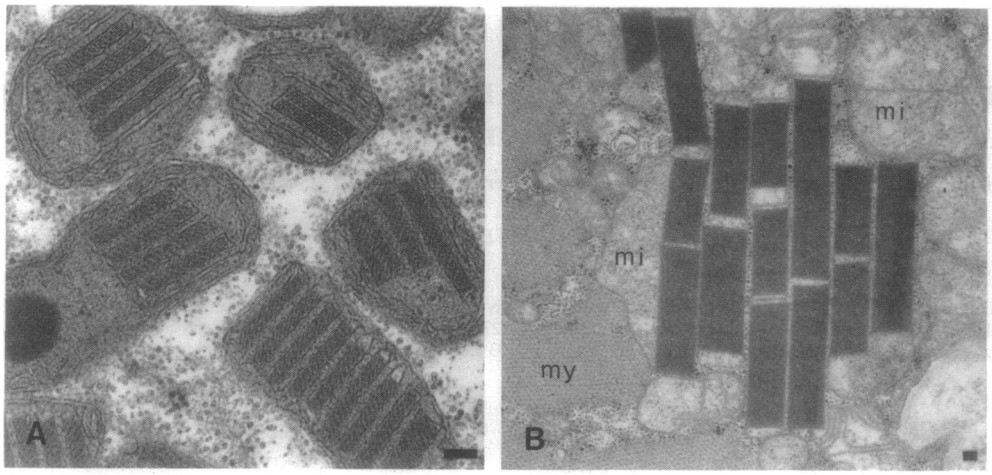

FIG. 1. Types of mitochondrial crystalline inclusions in human skeletal muscle biopsies. Muscle biopsies (quadriceps) were from a patient with CPEO (*A*) and a patient with a nonclassified mitochondrial myopathy (*B*). The biopsies were prepared according to standard electron microscopic procedures. (*A*) Morphological features of type I crystals. The basic structural unit of this type appears in thin sections as a rectangular unit, about 32 nm wide and of varying length, always located within the intracristal space (*A*) or in the outer compartment space between the inner and outer membrane. (*B*) Cluster of type II crystals. The crystal-like character of these inclusions, which are always present in the outer mitochondrial compartment, is far more pronounced than that of type I crystals. mi, Mitochondrion; my, myofibril. (Bars = 0.1 μm.)

Thin sections of tissue specimens, conventionally fixed and embedded for electron microscopy, were pretreated with sodium periodate, followed by the incubation procedure as applied to LR White embedded material. Controls were incubated either in the absence of primary antibody or with heterologous antibodies directed against proteins that are absent in skeletal muscular tissue. For Mi-CK enzyme cytochemistry, muscle tissue cryosections (30–40 μm) were treated according to Biermans *et al.* (13).

Image Processing. Specimens of human quadriceps muscle from patients with mitochondrial myopathies, in this case with CPEO, were fixed with 2% glutaraldehyde, postfixed with 2% OsO_4 and block-stained with 5% uranyl acetate, dehydrated through a graded series of ethanol and finally 100% acetone, embedded in Epon 812 resin, sectioned, and poststained with uranyl acetate and lead citrate (for details see ref. 8). Negatives (kindly provided by Sven Hovmöller, University of Stockholm) representing different areas of crystalline inclusions were inspected by laser diffraction. Areas showing most defined optical diffraction patterns with the highest resolution were chosen for further image processing. First, selected areas were digitized directly from the negative by an electronic camera (Datacopy 610F, Long Beach, CA). The pixel size was 25 μm corresponding to 0.67 nm at the specimen level. These digitally recorded areas of the crystalline inclusions were then processed with the standard SEMPER image processing system, and areas of 250 × 1000 pixels were averaged by crystallographic averaging (Fourier filtration) as described (14).

RESULTS AND DISCUSSION

The intramitochondrial inclusion crystals showed complete resistance to RNase treatment (Fig. 2*A*) but were sensitive to Pronase P digestion (15), indicating that they are of proteinaceous nature. This can be clearly seen in Fig. 2*B*, where electron-lucent "hollows" remain after Pronase P digestion. No immunoreactivity was found using antibodies against cytochrome *c* and cytochrome oxidase (COX), against the ATP/ADP-carrier, or against sera directed against nonmuscle proteins (results not shown).

Recently, Eppenberger-Eberhardt *et al.* (16) showed that adult rat cardiomyocytes, when cultured in creatine-free medium, displayed elongated mitochondria with intramitochondrial inclusions, quite similar to those observed in patient biopsies (7, 8). They also demonstrated that these crystalline inclusions were highly reactive with specific antibodies against the mitochondrial isoform of creatine kinase (Mi-CK) (17).

Mi-CK is a member of the creatine kinase (CK) isoenzyme family. In muscle and other cell types of high and fluctuating energy requirements, the CK isoenzymes are compartmentalized subcellularly. They play an important role in cellular energy homeostasis—e.g., for high-energy phosphate buffering, transport, and utilization and for fine-tuning and regulation of the cellular energy metabolism (for recent reviews see refs. 18 and 19). In normal mitochondria, Mi-CK is localized along the entire inner mitochondrial membrane (11, 12) as well as at the mitochondrial periphery where inner and outer mitochondrial membranes are in close apposition (20). Mi-CK was found to be enriched in isolated mitochondrial contact site fractions (21). Mi-CK is coupled to oxidative phosphorylation in the mitochondria (22–24). With its intricate octameric structure (11, 14, 17, 25), localization (12, 20, 21), and membrane interaction properties (26), Mi-CK is well suited to facilitate metabolic channeling of high-energy phosphates at the mitochondrial contact sites where the enzyme is functionally coupled to the ADP/ATP translocator of the inner and to porin of the outer mitochondrial membrane (22, 23, 27, 28). Mi-CK provides phosphocreatine (*P*Cr) as a source of high-energy phosphate to the cytosolic CKs, which are coupled to energy-consuming processes. Creatine then diffuses back to the mitochondria completing the *P*Cr shuttle (18, 19, 22, 29). The use of *P*Cr rather than ATP as the energy currency allows the cellular energy metabolism to be delicately regulated (18, 19, 27).

In sections of skeletal muscle biopsies from encephalomyopathy patients, numerous morphologically abnormal and enlarged mitochondria, some with intramitochondrial inclusions of different sizes, can be seen (Figs. 1 and 2 *C* and *D*). The formation of inclusions is always preceded by marked changes in cristae membrane disposition, with these membranes often taking a concentric arrangement (Fig. 1*A*). The question as to whether lipid peroxidation, presumed to be increased in patients with mitochondrial myopathies (3, 30), is involved in this reorganization of the membrane system remains to be answered.

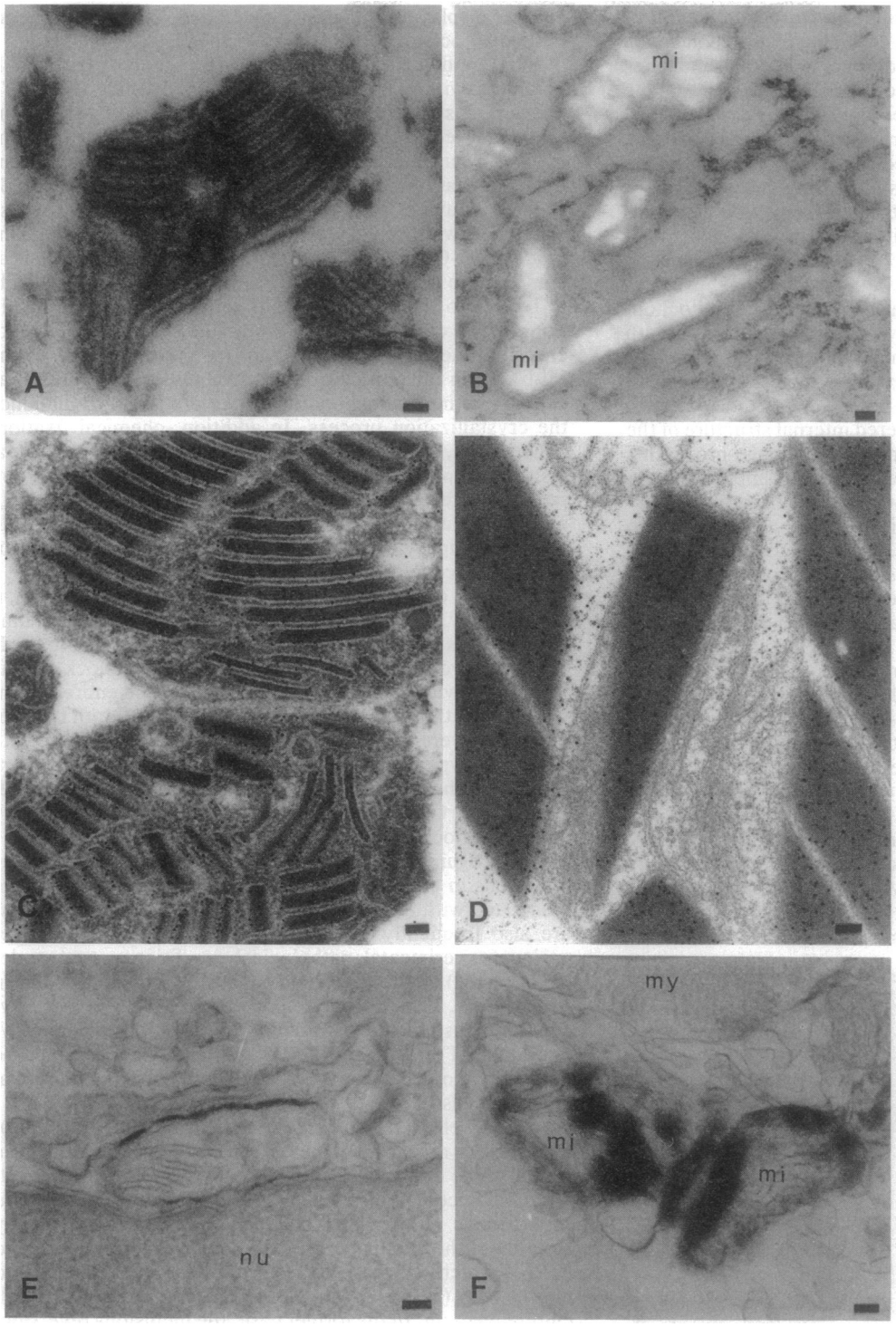

FIG. 2. Topochemistry of human mitochondrial crystalline inclusions. Skeletal muscle biopsies (quadriceps) were from CPEO (*A–C*), Kearns–Sayre (*D*), and MELAS patients (*E* and *F*). The biopsy specimens were prepared for digestion studies (*A* and *B*), immuno-electron microscopy (*B* and *C*), and enzyme cytochemistry (*E* and *F*) (13). Whereas RNase treatment (*A*) let the crystals undisturbed, Pronase treatment (*B*) caused complete digestion of the inclusions, leaving well-defined electron-transparent areas in the affected mitochondria. Such a proteolysis susceptibility indicates the overall proteinaceous nature of the crystals. (*C* and *D*) Distinct anti-Mi-CK immunoreactivity of type I (*C*) and strong anti-Mi-CK labeling of type II crystals (*D*), even demonstrable after conventional electron microscopic histological treatment of the muscle specimens. The strong and homogeneous goldlabeling of the entire crystals by the specific anti-Mi-CK antibody, even after the application of procedures that are known to seriously interfere with immunostainability, is taken to indicate a very high concentration of Mi-CK in the crystals. Mitochondria in RR fibers without inclusions show moderate Mi-CK enzyme activity in the intermembrane space beneath the outer mitochondrial membrane (*E*), but affected mitochondria (*F*) show strong enzyme activity beneath the outer mitochondrial membranes as well as in the interior of the organelles, presumably over the crystalline inclusions. mi, Mitochondrion; my, myofibril; nu, nucleus. (Bars = 0.1 μm.)

Within the mitochondria of different muscle fibers of these patients, two types of crystalline inclusions, type I crystals (Figs. 1*A* and 2 *A* and *C*) and type II crystals (Figs. 1*B* and 2*D*), are visible (for details see ref. 8). As visualized by immunogold staining, both crystal types were specifically and strongly decorated by well-characterized antibodies, specific for Mi-CK (11, 12, 16, 17, 20), with type II crystals always being somewhat more heavily labeled than type I crystals (compare Fig. 2*C* with 2*D*). Anti-Mi-CK labeling was uniform in both crystal types, irrespective of the orientation of the crystals to the plane of section. Without exception, all crystalline inclusions seen in our biopsy material were strongly labeled. Identical labeling of mitochondrial crystalline inclusions by anti-Mi-CK was observed in a biopsy specimen from a patient suffering from polymyositis (data not shown).

Except mitochondria, no other cellular structures or compartments were stained by this anti-Mi-CK antibody. The intensity of immunolabeling by anti-Mi-CK parallels inclusion formation. Mitochondria that showed reorganized cristae membranes in the absence of visible inclusions gave levels of immunostaining along the cristae membranes comparable in intensity and localization to those seen in normal mitochondria. Foci where crystal formation was being initiated were also distinctly labeled by anti-Mi-CK antibody (not shown). In mitochondria containing inclusions, the cristae membranes also showed more or less normal anti-Mi-CK staining, but the relative staining intensity of the inclusions

was drastically enhanced, indicating a net accumulation of Mi-CK in these mitochondria. The high immunolabeling intensity and the uniform distribution of gold grains indicates that Mi-CK is indeed a main component of the crystalline material. This is further corroborated by the fact that CK enzyme histochemistry (13) performed on frozen sections, subsequently embedded for electron microscopy, revealed high enzyme activity in the crystal-bearing mitochondria of RR fibers (Fig. 2*F*), indicating that Mi-CK is still enzymatically active in the affected mitochondria. We also found some staining of peripheral stretches just along or beneath the outer mitochondrial membrane (Fig. 2*E*), presumably representing contact sites (13), but in the pathological mitochondria a strong staining was always observed, either beneath the outer mitochondrial membrane or intramitochondrially—i.e., in the regions containing crystalline inclusions (compare Fig. 2*F* with 2*E*).

The large size periodically ordered internal structure of the crystalline inclusions allowed analysis by image processing (Fig. 3). The most suitable materials for this approach were the large sheet-like type II crystals, particularly when sectioned along the crystallographic *b, c* planes according to Farrants *et al.* (8) (see Fig. 3*A*). Digitally computed power spectra of selected areas of these type II crystals revealed reflections up to the second order (Fig. 3*B*). It has not been possible yet to obtain similarly large areas of planar sections along the *b, c* planes of type I crystals suitable for image processing. The lattice seen in Fig. 3*B* shows unit cell dimensions of 17.2 × 10.6 nm, which differ only slightly from the *b* and *c* vectors of the ortho-rhombic type II crystalline inclusions (17 and 8 nm, respectively) published earlier (8). Image processing yielded the averaged picture shown in Fig. 3*C*, displaying an arrangement of regular, ≈10-nm square particles with a central cavity. These structures and their arrangement are very reminiscent of isolated single Mi-CK octamers (14) and of Mi-CK octamers in protein crystals obtained with highly purified Mi-CK (25). In both cases, square-shaped (14) or windmill wheel-like structures (22) with exactly 10-nm sides and a central channel or indentation,

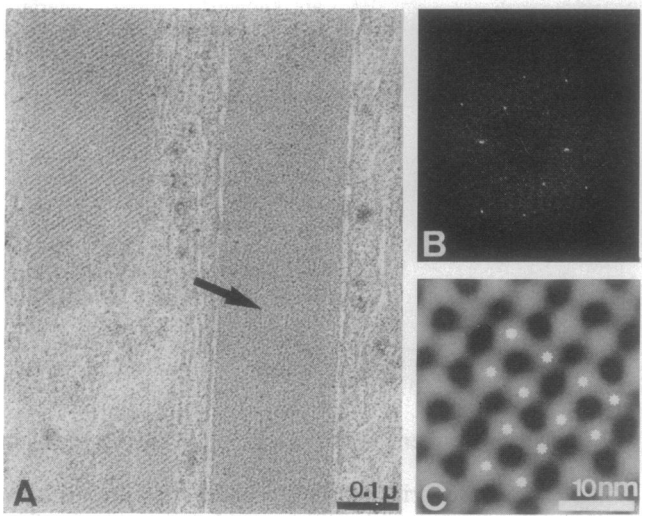

FIG. 3. Oriented sections through Mi-CK-rich mitochondrial inclusions reveal Mi-CK octamer motifs. (*A*) Selected view of a type II crystalline mitochondrial inclusion of a human quadriceps muscle biopsy from a patient with CPEO. The area indicated by the black arrow, representing a section along the *b, c* planes, gave a rather defined optical diffraction pattern (*B*) and was therefore chosen for digitization. Computerized image processing of the crystal area indicated by the arrow in *A* resulted in the averaged image shown in *C*. Three individual octamers showing side widths of 10 × 10 nm and a central cavity are outlined by white asterisks, and a corresponding packing mode is suggested.

such as displayed in Fig. 3*C*, have been shown to represent individual octameric Mi-CK molecules.

Even though the suggested packing mode of the Mi-CK octamers within the type II inclusion crystals (Fig. 3*C*), showing a staggered arrangement, differs somewhat from that observed in the pure Mi-CK protein crystals (25), the results of our image processing of the inclusions are strong evidence that type II crystals are indeed composed of highly ordered arrays of square-shaped Mi-CK octamers that also show side widths of 10 nm. The difference in the packing mode of Mi-CK molecules in the *in vivo* inclusion crystals as compared to the *in vitro* Mi-CK protein crystals is very likely to be due to the completely different crystallization conditions. For example, *in vivo*, the binding of Mi-CK to mitochondrial membranes (24, 26) and/or the interaction of the Mi-CK with membrane proteins (for review see ref. 19) as well as the intramitochondrial milieu are likely to influence the crystallization process. In addition, chemical fixation, dehydration, and sectioning may lead to slight artifactual distortions of the lattice parameters. Lipid peroxidation, possibly affecting the known interaction of Mi-CK with mitochondrial membranes and phospholipids (26), especially with cardiolipin (24, 31), has also to be considered as a factor of importance in the induction of crystal formation.

Taking all our results together, we believe that the main, if not the only, component of both types of these crystalline inclusions is indeed Mi-CK. Image processing of type II crystals revealed a single type of building block in the inclusions, with dimensions and general shape entirely compatible with those of Mi-CK octamers (Fig. 3). Both types of inclusions were labeled with antibodies against Mi-CK, with labeling of type II crystals being somewhat stronger (compare Fig. 2*D* with 2*C*). Finally, CK enzyme histochemistry revealed high CK enzyme activity within the pathologically affected mitochondria (Fig. 2*F*).

It is intriguing that Mi-CK should accumulate as crystalline inclusions in patients with those mitochondrial myopathies associated with RR fibers (1, 7, 8, 19). Analogous inclusions are also frequently observed in laboratory animals under various experimental pathological conditions—e.g., under ischemia (32) or after depletion intracellular creatine levels in muscle (refs. 33 and 34 and references therein). Interestingly, similar inclusions are also induced by 3′-azido-3′-deoxythymidine (AZT) treatment of AIDS patients (35). It should be interesting to see whether or not these intramitochondrial inclusions also turn out to be Mi-CK crystals.

Muscle cells must import creatine from the serum (36). When adult rat cardiomyocytes are grown in creatine-free medium, the cytosolic creatine and *P*Cr pools are depleted, and Mi-CK-containing inclusions are induced within a period of 4–5 days (16). The same phenomenon is observed by addition of the creatine analogue, β-guanidinopropionic acid (GPA), which is known to block the entry of creatine into muscle cells (36), even in the presence of creatine in the cell culture medium. In the former case, the inclusions reversibly disappear within a few days after addition of creatine to the cell culture medium (16). In an animal model, rats fed GPA for a prolonged period of time also develop Mi-CK-containing mitochondrial inclusions, which disappear again after the cessation of GPA administration (37).

The formation of mitochondrial inclusions in creatine-deficient cardiomyocytes and in GPA-fed rats may be explained by functional impairment of the cytosolic part of the CK/*P*Cr system, causing a metabolic overcompensation at the mitochondrial side of the *P*Cr circuit, which results in an overaccumulation of Mi-CK. Accumulated Mi-CK then leads to inclusion formation. Interestingly, in a recent study of CPEO patients, Mi-CK activity was clearly enhanced in muscle samples of the two patients whose biopsies were positive for inclusions but not in the others' biopsies, where

no inclusions were found. On the other hand, no clear trend between the occurrence of inclusions and lowered concentration of total, free, or phosphorylated creatine has been found in the few patients investigated so far (38).

We propose that the Mi-CK-rich inclusions seen in patients with mitochondrial myopathies associated with the RR fiber pathology are formed as a response to a cytosolic low-energy stress situation and that their appearance may not necessarily be caused primarily by specific defects within the mitochondrial metabolism itself. Seen in this light, the inclusions would be a secondary consequence of as yet unidentified defects either at the producing or the consuming side of energy metabolism, either on the substrate or on the corresponding enzyme level. This hypothesis is an attractive way to explain syndromes like CPEO, Kearns–Sayre, MELAS, and other mitochondrial myopathies where the primary defects are not known precisely yet and where Mi-CK-rich inclusions are always prominent.

Whether the inclusions serve a compensatory ameliorative function—e.g., by increasing the export of high-energy phosphates from the mitochondria, compatible with the proposed function of Mi-CK as an energy-channeling molecule (19, 27, 29)—remains to be determined. It is reasonable to assume that this may be true at least transiently. Overexpression and subsequent accumulation of Mi-CK in the intermembrane space, induced by metabolic stress, could initially improve energy transport but subsequently, after a certain threshold concentration of Mi-CK is reached, cause a spontaneous crystallization of the enzyme leading to pathological accumulations of Mi-CK crystals. This is in accordance with the observation that purified Mi-CK has been shown to readily form filaments or sheet-like structures *in vitro* and that Mi-CK is very stable in its crystalline form (14, 25). Even though Mi-CK is enzymatically active under these circumstances, crystallization of the enzyme between cristae membranes or between inner and outer membrane would seem unlikely to improve the functional coupling of Mi-CK with the ATP/ADP translocator of the inner and with porin of the outer mitochondrial membrane (28). But nevertheless, the presence of Mi-CK-rich inclusions may turn out to be a valuable indicator for a number of deficiencies in cellular energy supply, caused by a variety of defects. In addition, the unique overcompensation of the CK system, seen as a common denominator in a variety of mitochondrial myopathies and in animal models, seems to point to the physiological importance of the CK/*P*Cr system for cellular energetics. This has recently been fully confirmed by the group of Bé Wieringa (University of Nijmegen), who demonstrated that transgenic mice lacking expression of cytosolic M-CK show a phenotype with markedly reduced burst activity of muscle contraction (39).

We are grateful to Dr. Sven Hovmöller (University of Stockholm, Sweden) for providing EM negatives of earlier work. We thank Dr. J. Tager (University of Amsterdam, The Netherlands) for the kind gift of the various cytochrome *c* and COX antibodies and Dr. M. Klingenberg (University of Münich, Germany) for the gift of ADP/ATP carrier antibodies. The skillful technical assistance of Huib Croes (Department of Cell Biology and Histology, University of Nijmegen) is greatly acknowledged. All members of the CK group of The Institute for Cell Biology in Zürich are acknowledged for helpful comments and discussion. Special thanks go to Dr. Elizabeth Furter-Graves, Dr. Markus Wyss, and Dr. David Iles for critical comments on the manuscript. This work was financially supported by the Swiss National Science Foundation (Grant 31-33907.92 to T.W.) and by a grant from the Swiss Foundation for Muscle Diseases (to T.W.) as well as by the Dutch Foundation for "Kinderen die wel willen maar niet kunnen" (to A.M.S.).

1. DiMauro, S., Bonilla, E., Zeviani, M., Nakagawa, M. & DeVivo, D. (1985) *Ann. Neurol.* **17**, 521–538.
2. Zeviani, M., Bonilla, E., DeVivo, D. & DiMauro, S. (1989) *Neurol. Clin.* **7**, 123–156.
3. Wallace, D. C. (1992) *Annu. Rev. Biochem.* **61**, 1175–2212.
4. Scholte, H. R. (1988) *J. Bioenerg. Biomembr.* **20**, 161–191.
5. Morgan-Hughes, J. A., Schapira, A. H., Cooper, J. M., Holt, I. J., Harding, A. E. & Clark, J. B. (1990) *Biochim. Biophys. Acta* **1018**, 217–227.
6. Stadhouders, A. M. (1981) in *Mitochondria and Muscular Diseases*, eds. Busch, H., Jennekens, F. & Scholte, H. (Mefar, Beesterzwaag, The Netherlands), pp. 113–132.
7. Stadhouders, A. M. & Sengers, R. C. A. (1987) *J. Inherited Metab. Dis.* **10**, Suppl. 1, 62–80.
8. Farrants, G., Hovmöller, S. & Stadhouders, A. M. (1988) *Muscle Nerve* **11**, 45–55.
9. Stadhouders, A., Jap, P. & Wallimann, T. (1990) *J. Neurol. Sci.* **98**, 304 (abstr.).
10. Stadhouders, A., Jap, P., Winkler, H. P. & Wallimann, T. (1992) *J. Muscle Res. Cell Motil.* **13**, 255 (abstr.).
11. Schlegel, J., Zurbriggen, B., Wegmann, G., Wyss, M., Eppenberger, M. H. & Wallimann, T. (1988) *J. Biol. Chem.* **263**, 16942–16953.
12. Wegmann, G., Huber, R., Zanolla, E., Eppenberger, H. M. & Wallimann, T. (1991) *Differentiation* **46**, 77–87.
13. Biermans, W., Bakker, A. & Jacob, W. (1990) *Biochim. Biophys. Acta* **1018**, 225–228.
14. Schnyder, T., Gross, H., Winkler, H. P., Eppenberger, H. M. & Wallimann, T. (1991) *J. Cell Biol.* **112**, 95–101.
15. Sluga, E. & Monneron, A. (1970) *Virchows Arch. Pathol. Anat.* **350**, 250–260.
16. Eppenberger-Eberhardt, M., Riesinger, I., Messerli, M., Schwarb, P., Müller, M., Eppenberger, M. H. & Wallimann, T. (1991) *J. Cell Biol.* **113**, 289–302.
17. Schlegel, J., Wyss, M., Schürch, U., Schnyder, T., Quest, A., Wegmann, G., Eppenberger, H. M. & Wallimann, T. (1988) *J. Biol. Chem.* **263**, 16963–16969.
18. Wallimann, T., Wyss, M., Brdiczka, D., Nicolay, K. & Eppenberger, M. H. (1992) *Biochem. J.* **281**, 21–40.
19. Wyss, M., Smeitink, J., Wevers, R. & Wallimann, T. (1992) *Biochim. Biophys. Acta* **1102**, 119–166.
20. Wegmann, G., Zanolla, E., Eppenberger, M. H. & Wallimann, T. (1992) *J. Muscle Res. Cell Motil.* **13**, 420–435.
21. Kottke, M., Adams, A., Wallimann, T., Kumar Nalam, V. & Brdiczka, D. (1991) *Biochim. Biophys. Acta* **1061**, 215–225.
22. Jacobus, W. (1985) *Annu. Rev. Physiol.* **47**, 707–725.
23. Saks, V., Kuznetsor, A., Kuprianov, A., Miceli, M. & Jacobus, W. (1985) *J. Biol. Chem.* **260**, 7757–7764.
24. Rojo, M., Hovius, R., Demel, R., Wallimann, T., Eppenberger, M. H. & Nicolay, K. (1991) *FEBS Lett.* **281**, 123–129.
25. Schnyder, T., Winkler, H. P., Gross, H., Eppenberger, H. M. & Wallimann, T. (1991) *J. Biol. Chem.* **266**, 5318–5322.
26. Rojo, M., Hovius, R., Demel, R., Nicolay, K. & Wallimann, T. (1991) *J. Biol. Chem.* **266**, 20290–20295.
27. Wyss, M. & Wallimann, T. (1992) *J. Theor. Biol.* **158**, 129–132.
28. Brdiczka, R. (1991) *Biochim. Biophys. Acta* **1071**, 291–321.
29. Bessman, S. & Carpenter, C. (1985) *Annu. Rev. Biochem.* **54**, 831–862.
30. Bindoli, A. (1988) *Free Radical Biol. Med.* **5**, 247–261.
31. Müller, M., Moser, R., Cheneval, D. & Carafoli, E. (1985) *J. Biol. Chem.* **262**, 3839–3843.
32. Hanzliková, V. & Schiaffino, S. (1977) *J. Ultrastruct. Res.* **60**, 121–133.
33. Gori, Z., DeTata, V., Pollera, M. & Bergamini, E. (1988) *Br. J. Exp. Pathol.* **69**, 639–650.
34. Ohira, Y., Kanzaki, M. & Chen, C. (1988) *Jpn. J. Physiol.* **28**, 159–166.
35. Dalakas, M., Illa, I., Pezeshkpour, G., Laukatis, J., Cohen, B. & Griffin, J. (1990) *New Engl. J. Med.* **322**, 1098–1105.
36. Fitch, C. D., Jellinek, M. & Mueller, E. J. (1974) *J. Biol. Chem.* **249**, 1060–1063.
37. Riesinger, I., Haas, C. & Wallimann, T. (1992) *Biochim. Biophys. Acta*, European Bioenergetics Conference short reports 7, 140A (abstr.).
38. Smeitink, J., Stadhouders, A., Sengers, R., Ruitenbeek, W., Wevers, R., ter Laak, H. & Trijbels, F. (1992) *Neuromuscular Dis.* **2**, 35–40.
39. Van Deursen, J., Heerschap, A., Oerlemans, F., Ruitenbeek, W., Jap, P., ter Laak, H. & Wieringa, B. (1993) *Cell* **74**, 621–631.